Investigation of a decentralised control strategy for grid frequency support from DC microgrids

A Florida-James[†], S Yana[†], A Emhemed[†], G Burt[†]

[†] Institute for Energy and Environment,, University of Strathclyde, Glasgow, UK
anthony.florida-james@strath.ac.uk[†], syiska.yana@strath.ac.uk[†], abdullah.emhemed@strath.ac.uk[†], graeme.burt@strath.ac.uk[†]

Keywords: DC microgrid, decentralised control strategy, grid frequency support

Abstract

DC microgrids are capable of integrating and coordinating distributed energy resources into power systems, along with providing services to the wider system e.g. balancing, frequency support, demand response, etc. This paper investigates the capability of DC microgrids providing grid frequency support, for the GB Enhanced Frequency Response service. In this study, photovoltaic generation, energy storage, and load, form the DC microgrids. The control strategy is a decentralised scheme, based on conventional droop control for active power sharing and grid frequency support. Droop control is also used within the DC microgrid for power sharing amongst generation and load. Scenarios are conducted to evaluate the effectiveness of the control strategy and verified by MATLAB/Simulink simulations.

1 Introduction

Moving towards a low carbon economy has stimulated increased uptake of distributed energy resources (DERs), such as photovoltaic (PV) generation systems, wind-based generation, and energy storage. Compared to AC microgrids, DC microgrids are a promising solution that can facilitate the adoption of such devices in a more efficient and controllable way. Many DER units natively generate DC and can be directly connected within a DC microgrid (DC-MG), thus eliminating the DC-AC conversion stages [1]. The control and operation of a DC-MG is less complex when compared to that of an AC microgrid (AC-MG). The general benefits of DC-MGs when compared to AC microgrids are [1]–[3]:

1. higher efficiency and reduced losses due to the reduction of multiple converters used for DC loads;
2. easier integration of various DERs, such as energy storage, solar PV, and fuel cells, with direct or reduced voltage conversion stage interfaces;
3. more efficient supply of DC loads, such as electric vehicles, LED lights, and other electronic devices;
4. eliminating the need for synchronising generators, which enables rotary generating units to operate at their own optimum speed; and
5. enabling bus ties to be operated with reduced fault levels and without the need for synchronising the buses.

Furthermore, due to simpler operation, a higher level of automation and enhanced control within a DC-MG can be achieved. Fully utilising this advantageous functionality can ensure the provision of ancillary services at the point of common coupling (PCC) to the AC grid. At the PCC the DC-AC voltage source converter (VSC) is situated. Therefore, whilst in grid connected mode, the bidirectional VSC and control strategy plays an important role in providing these ancillary services. The DC-MG control strategy must also manage the energy requirements within the DC-MG. Without proper energy management on the DC side, the grid services cannot be provided to the main AC grid. With conventional fossil-fuel based generation reducing, frequency support services provided by VSC interfaced generation is increasingly important. Previous studies have investigated providing frequency support by using wind turbines, PV generation, and energy storage [4]–[6]. PV and battery storage generate DC natively. However, only a few studies have investigated the possibility of using a DC-MG for grid frequency support [7]. One challenge is a lack of rotating mass, or characteristics of the DER, e.g. semiconductor technology used for PV, which makes the DER within the DC-MGs decoupled from the grid [8]. This condition makes it difficult for DERs to emulate the inertia response of a synchronous machine, without using advanced control strategy. Furthermore, with a decrease in overall system inertia, higher rate-of-change-of-frequency (RoCoF) will occur

Therefore, this paper investigates the capability of a DC-MG utilising the collective active response of its DERs, to provide wider system frequency support. In the GB network, it is possible for DERs $\geq$ 1 MW to participate in the enhanced frequency response (EFR) service [9]. The performance of one DC-MG is evaluated whilst participating in this service. A second DC-MG is introduced to evaluate the impact of different DC-MG demand on the host network, in terms of the EFR and energy management within the DC-MG. Controller interactions between two DC-MGs operating in opposing modes are studied. Issues with modelling and scalability are presented, along with consideration of DC-MG design requirements to enable EFR participation. The paper is organised as follows: Section 2 provides a review of existing DC-MG control strategies. Section 3 describes the modelling of DC-MGs and the utilised decentralised control strategy for grid frequency support. Section 4 presents the discussion and evaluation of the DC-MG decentralised control strategy and

simulation studies. Section 5 presents the conclusions from the study.

2 Review of existing DC microgrid control strategies

In general, there are three types of DC-MG control strategies: centralised, distributed and decentralised [10]. A centralised control strategy operates by using direct communication links between the central control unit (CCU) and all controllable devices. In this strategy, all the data from DERs and controllable devices within the DC-MG are collected then sent to the CCU. Then, based on this system information the CCU makes control decisions and sends the commands to each unit within the system. A centralised approach provides a good system-wide performance, and typically provides the most optimal solution for secondary control actions. However, this method has disadvantages if there is severe communication delays or link failure, CCU failure, or potential cyber security issues [1], [10].

Distributed control schemes also use multiple communication links but do not require a CCU. Distributed control schemes typically share control responsibility amongst multiple units, as seen in consensus algorithm based approaches [11]. The communication links are between the DERs [10], thus proving to be more resilient during communication link failure. However, control actions with these distributed schemes can be slower and less optimal than centralised approaches due to the requirement for consensus and the possibility for sparse communication link topologies to cause delays [12].

The last control strategy is decentralised control, which has been widely applied in AC microgrids and DC-MGs research [13]. Unlike centralised and distributed control strategies, this control strategy does not rely on communication links. Decentralised control is assumed to be less complex than other control strategies [10]. However, most of the research has primarily focused on voltage regulation and power sharing among DER units within the microgrid [14], [15]. Therefore, this study focuses on the investigation of DC-MG for grid frequency support through a decentralised control strategy. The network model and control strategy used in this work is outlined in the following section.

3 Modelling of DC microgrid decentralised control strategy for grid frequency support

This section first outlines the DC-MG test network and the parameters used for this study. Section 3.2 outlines the control strategy which enables the DC-MG to provide the EFR frequency support service.

3.1 Test network

The DC-MG model used in this study comprises of PV, energy storage and load which is connected to the DC bus, as shown in Figure 1. The DC-MG connects to the main grid through an 11kV/0.4 kV transformer for galvanic isolation, and then an AC-DC converter. The representative host power system in this study is modelled by using a dynamic 350 MVA synchronous machine. The synchronous generator set utilises an IEEE Type 1 Excitation system and a turbine/governor model to enable AC system frequency deviations following an event. To create a frequency event in the AC side, a load step change is created at AC load-1 on the 11 kV side. Both of the DC-MGs have the same units and parameters, which are shown in Table 1.

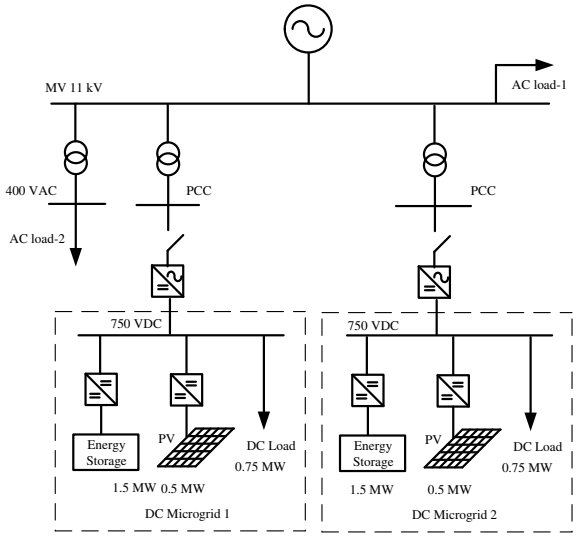

Figure 1: Test network used for simulation studies

System parameters	
Synchronous machine	350 MVA, 11 kV, 50 Hz
Transformers	5 MVA, 11/0.4 kV, 50 Hz
Load step changer	30 MW
AC load in 11 kV side	250 MW and 0.5 MW
AC load in 0.4 kV side	24.23 kW, 10.43 kVAR
AC-DC Converter Rating	1 MW
DC Voltage	750 VDC
Battery	1.5 MW
PV	0.5 MW
DC load	0.75 MW

Table 1: System parameters

The DERs in each DC-MG are connected to a 750 VDC bus. This enables connection with the three phase 400 VAC grid and provides higher power transmission capacity on the DC link, when compared to an equivalent AC system [16], [17]. Due to the relatively short time of the simulation, the PV was assumed to generate constant power without disturbances from temperature and irradiance. However, the short term effects of irradiance and temperature on the PV generation can be investigated in future work, as a representative PV model [18] was integrated for these studies. The battery used in this simulation is a Lithium-Ion Battery model found within MATLAB with a nominal voltage of 600 Vdc, and an initial

SOC of 80%. The battery is connected to the DC bus through a detailed bidirectional DC-DC buck boost converter model.

3.2 Control strategy

There are three power converters used per DC-MG. As shown in Figure 1, the power converters in the test network are: the main bidirectional VSC, energy storage bidirectional DC-DC 'buck-boost' converter and PV unidirectional DC-DC 'boost' converter. The AC-DC converter control is shown in Figures 2-3, with the DC converter control shown in Figure 4.

3.2.1 AC-DC converter control

The control strategy for the VSC utilises vector current control, which consists of an outer power control loop, and an inner current control loop.

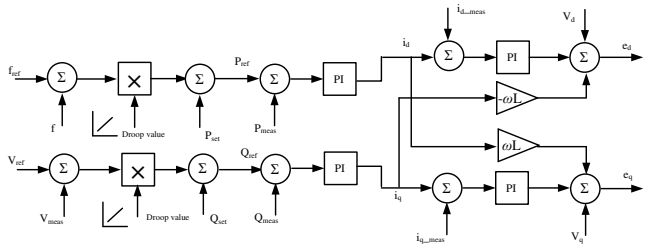

Figure 2: VSC Vector Current Control Utilised

VSC controller parameters	
Switching frequency (f_{sw})	2 kHz
Filter parameters:	
R_f	1.2 mΩ
L_f	1.6 mH
Inner loop gain:	
k_i	38
k_p	4
Outer loop gain:	
k_i	25
k_p	0.05

Table 2: VSC controller parameters

The proportional and integral (PI) gains for the inner loop were calculated based on the system parameters using [19]:

$$k_p = \alpha_c \times L_f / Z_s \quad (1)$$

$$k_i = \alpha_c \times R_f / Z_s \quad (2)$$

Where Z_s = system base impedance (Ohms), L_f = AC filter inductance (H), and R_f = filter resistance (Ohms). The desired bandwidth of the inner control loop, α_c, is calculated by

$$\alpha_c = (f_{sw} / 5) \times 2\pi \quad (3)$$

The active and reactive power setpoints are determined by the droop curve, and also a steady-state controller whilst the frequency lies within the narrow deadband as seen in Figure 4. Therefore, two levels of droop control are implemented for AC side control actions. First, whilst the main grid is in steady-state operating conditions we assume that 49.985 Hz < f_n < 50.015 Hz. Whilst the AC frequency is within this EFR droop deadband, the DC-MG may wish to export or absorb power from the main grid. However, the power consumption or absorption by the DC-MG may cause the frequency to deviate outside of the deadzone in this case study, due to the base load conditions and the size of the DC-MG relative to the host grid. Although a 1 MW DC-MG will not have this much of an effect in a real network, multiple DC-MGs may cause this effect, especially in a future network scenario where there is reduced inertia for example. Therefore, the following droop-based decentralised control modes at the AC-DC converter are used, whilst the system is within steady-state bounds:

1) Mode 1 (Self-consumption): the DC-MG does not inject or absorb power from the main grid whilst in this mode.

2) Mode 2 (Import mode): the DC-MG absorbs power from the grid whilst the frequency is within the deadzone bounds.

3) Mode 3 (Export mode): the DC-MG injects power to the grid whilst the frequency is within the deadzone bounds.

By using these droop-based modes, power can still be consumed or injected by the DC-MG when there is no frequency event that requires the response as stipulated by the EFR service. This also means that, in a stiffer grid, the DC-MG primary controller enables the consumption or absorbtion up to ± 1pu when f = 50 ±0.015 Hz. The power setpoint limits and mode selection by the AC-DC converter can be determined by means of DC-bus signalling [20], which is outside the scope of this work. When f is outside the deadband, the DC-MGs participate in the EFR service, a narrow deadband droop is used, with a 1% droop curve percentage, as shown in Figure 3.

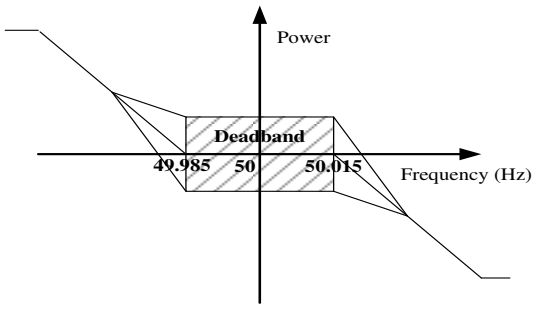

Figure 3: Service envelope [21]

3.2.2 DC converter control

The battery utilises a V-I droop control for the buck-boost DC-DC converter. When the AC frequency deviates, the voltage in DC side deviates respectively due to active power demand i.e.

a VSC power reference $P_{ref} > 0$ causes a drop in the DC voltage, and vice-versa. When the DC voltage reduces slightly, the battery will inject the current into the DC bus. Figure 5 shows the block diagram of buck-boost DC-DC converter and the controller. This control strategy enables power sharing among the DER units within DC-MG, thus managing energy requirements within the DC-MG. Note that the SoC-adaptive control can be selected to on or off by the battery, depending on the power requirements within the microgrid i.e. it can be initiated when total power output of battery rated power not required but SoC is low/high.

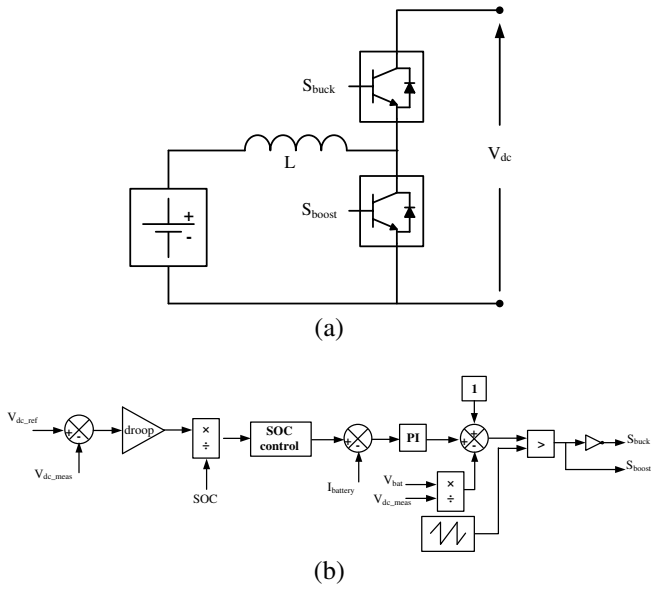

Figure 4: (a) Buck-boost DC-DC converter, (b) Controller

DC-DC Buck-boost parameters	
Droop gain	12
Proportional gain	12
Integral gain	25
Switching frequency	1 kHz
Inductor	2 mH

Table 3: Buck-Boost Parameters

4 Simulation studies evaluation of DC microgrid decentralised control strategy

The DC-MG test network and control strategy was tested by using MATLAB/Simulink software. The simulations tested the performance of DC-MG and control strategy during steady state conditions, the response to a system frequency event at t =15 s, and the transition between the different control modes. There are three scenarios implemented to test the DC-MG and control strategy performance in this study. Case study 1 utilises one DC-MG operating in the three different pre-event modes, as outlined in Section 3.2.1. For Case Study 1 the annotation for the modes are CS1.1 for Mode 1, CS1.2 for Mode 2, and CS1.3 for Mode 3. Case study 2 utilises two DC-MGs operating in the same modes pre-event (CS2.1 – CS2.3) and also for the case where the DC-MGs utilise opposing pre-event modes, where DC-MG_1 exports and DC-MG_2 exports before the frequency event. (CS2.4). The following sub-sections will present the simulation results for and discussion.

4.1 Case study 1

For CS1.1, the loads in the microgrid are supplied by local resources. Figure 5 shows the response of the microgrids at t = 15s a grid frequency event occurs.

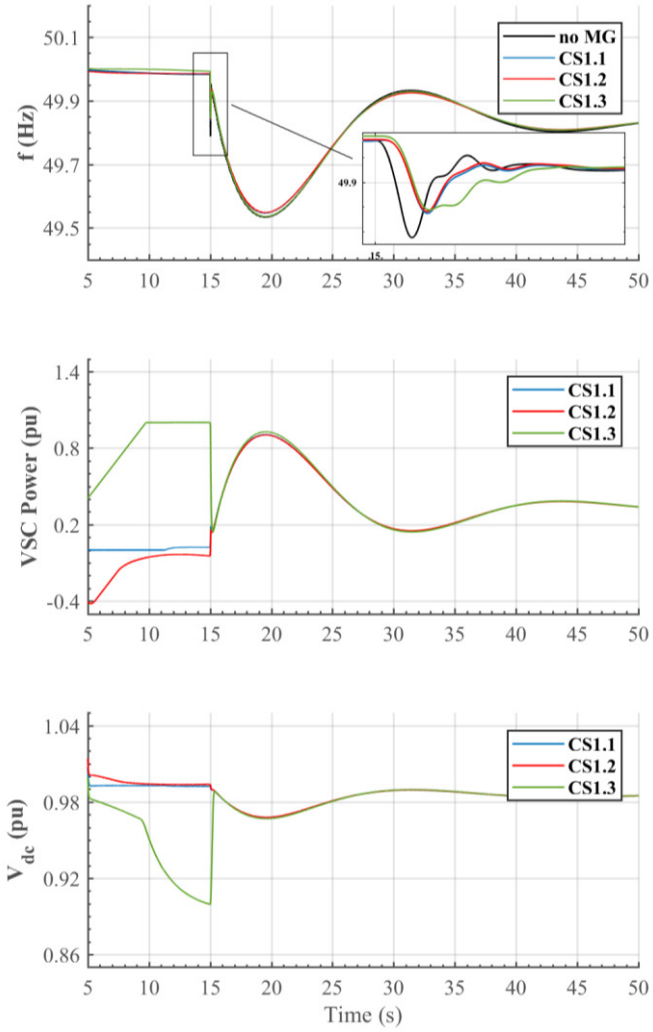

Figure 5: (a) MG_1 data for CS1.1-3

4.2 Case study 2

In this case, results are presented for the case of two DC-MGs. Four scenarios were investigated, where the same three steady-state modes were used by each DC-MG. As previously mentioned, for CS2.4, one DC-MG VSC power control scenario was considered, where one DC-MG imports pre-event, and the other DC-MG exports pre-event. In this study PV power output is set to 0.6 pu of the rated power output, and is therefore providing 300 kW. Therefore, due to the DC-MG design, the VSC can still export 1 MW, which is part of the minimum requirement as an EFR service provider [9].

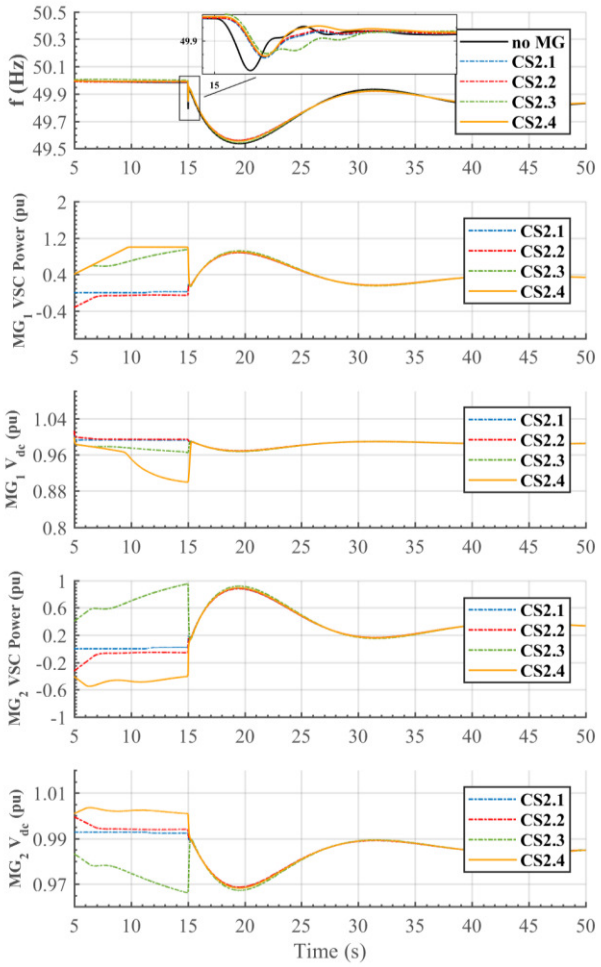

Figure 6: Results for two DC-MGs, pre-event modes and frequency response following event at t = 15 s

4.3 Discussion

Case study 1 demonstrates that the VSC is capable of responding as expected, whilst the DC control meets the energy requirements within the DC-MG. Even with one DC-MG, there is an improvement in the initial frequency deviation when compared to the system response without any DC-MGs, as seen in Figure 5. From Figure 7, it is evident that there is an improvement in the RoCoF for all pre-event VSC modes. The pre-event mode that provides the fastest frequency response is the export mode (CS1.3). However, due to the ramping down of VSC power when transitioning into the EFR droop, the nadir is larger when compared to the import mode (CS1.2). It is important to note the slight difference in VSC power exported during the frequency event. This is due to the impact of the pre-event power control action, where it can be seen the reduction of VSC power export, causes the frequency to deviate further from nominal. This means that for CS1.3, the VSC has to export more power compared to CS1.2. From this, further work will explore the alternative 'smart' control schemes, whereby the transition from the pre-event control mode to frequency event EFR service mode does not require more power from the DC-MG.

For Case Study 2, the import pre-event mode (CS2.2) is shown to enable a greater primary response and to improve the frequency nadir. For CS2.4, the frequency nadir is also improved when compared to CS2.3 but has a slower initial response which is likely due to the effect of MG_1 ramping down at the detection of the frequency event.

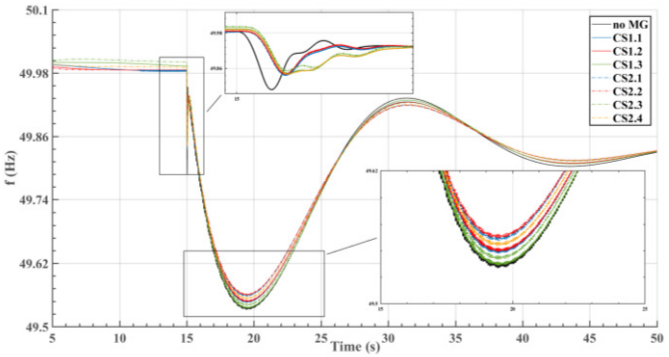

Figure 7: Frequency response for all scenarios.

Another important observation from the study is the comparison of initial frequency response and nadir for CS1.1 and CS1.2 to CS2.3. Even though two DC-MGs are connected for CS2.3, the responses from CS1.1 and CS2.2 are not as effective as CS1.1 and CS1.2, where only one DC-MG is connected. Lastly, the control approach implemented for steady-state power sharing is shown to provide support between DC-MGs, as seen for the case of CS2.4 in Figure 6. For example, when compared to Case study 1 results, the DC-MG_1 enables DC-MG_2 to absorb more power whilst in import mode. This control scheme could thus facilitate a level of co-operation amongst neighbouring DC-MGs, locally clustered together. Further research into DC-MG decentralised control will explore this possibility and address the main VSC controller issue experienced with the transition between control modes, as seen for CS1.3 and CS2.3. Further tests of the frequency support capability will also be investigated, such as response time and alternative local VSC control schemes.

5 Conclusions

This study investigates the opportunity for DC-MG to provide grid frequency support. The droop-based decentralised DC-MG and VSC control strategy was implemented, and enabled the DC-MGs to provide AC frequency support to the host network. The case study simulation results show that the control strategy succeeds in the expected response as per the droop curve stipulated by the EFR service. The control strategy not only enables grid-support by active power injection to or absorption from the grid but also maintains the power sharing amongst DERs within the DC-MG. Future work will involve further testing of the response for the EFR service and also improve transition between VSC control modes. Any DC link issues, such as power sharing during low PV generation and short term irradiance/temperature deviations, will also be investigated. This will inform further studies into DC-MG and control strategy will be developed as to ensure provision of

frequency support without detrimentally effecting DC-MG operation.

Acknowledgements

The authors would like to acknowledge support from the EPSRC CDT in Future Power Networks and Smart Grids. This study was also supported by LPDP (Indonesia Endowment Fund for Education) and Indonesia Ministry of Research, Technology and Higher Education (RISTEK DIKTI) through the BUDI-LN scheme.

References

[1] D. Kumar, F. Zare, and A. Ghosh, "DC Microgrid Technology: System Architectures, AC Grid Interfaces, Grounding Schemes, Power Quality, Communication Networks, Applications and Standardizations Aspects," IEEE Access, pp. 1–1, 2017.

[2] J. Ma, L. Yuan, Z. Zhao, and F. He, "Transmission Loss Optimization-Based Optimal Power Flow Strategy by Hierarchical Control for DC Microgrids," IEEE Trans. Power Electron., vol. 32, no. 3, pp. 1952–1963, Mar. 2017.

[3] T. Dragicevic, X. Lu, J. C. Vasquez, and J. M. Guerrero, "DC Microgrids-Part II: A Review of Power Architectures, Applications, and Standardization Issues," IEEE Trans. Power Electron., vol. 31, no. 5, pp. 3528–3549, May 2016.

[4] Y. Fu, Y. Wang, and X. Zhang, "Integrated wind turbine controller with virtual inertia and primary frequency responses for grid dynamic frequency support," pp. 1129–1137, 2017.

[5] A. Hoke, M. Shirazi, S. Chakraborty, E. Muljadi, and D. Maksimovic, "Rapid Active Power Control of Photovoltaic Systems for Grid Frequency Support," IEEE J. Emerg. Sel. Top. Power Electron., pp. 1–1, 2017.

[6] D. Gladwin et al., "Battery energy storage systems for the electricity grid: UK research facilities," in 8th IET International Conference on Power Electronics, Machines and Drives (PEMD 2016), 2016, p. 6 .-6 .

[7] D. Chen, Y. Xu, and A. Q. Huang, "Integration of DC Microgrids as Virtual Synchronous Machines into the AC Grid," IEEE Trans. Ind. Electron., pp. 1–1, 2017.

[8] X. Lyu, Z. Xu, J. Zhao, and K. P. Wong, "Advanced frequency support strategy of photovoltaic system considering changing working conditions," IET Gener. Transm. Distrib., vol. 12, no. 2, pp. 363–370, 2018.

[9] National Grid, "Enhanced Frequency Response," 2016.

[10] T. Dragicevic, X. Lu, J. Vasquez, and J. Guerrero, "DC Microgrids-Part I: A Review of Control Strategies and Stabilization Techniques," IEEE Trans. Power Electron., pp. 4876–4891, 2016.

[11] M. Yazdanian and A. Mehrizi-Sani, "Distributed Control Techniques in Microgrids," IEEE Trans. Smart Grid, vol. 5, no. 6, pp. 2901–2909, 2014.

[12] Y. Wang et al., "Aggregated energy storage for power system frequency control: a finite-time consensus approach," IEEE Trans. Smart Grid, 2018.

[13] X. Lu, K. Sun, J. M. Guerrero, J. C. Vasquez, and L. Huang, "State-of-Charge Balance Using Adaptive Droop Control for Distributed Energy Storage Systems in DC Microgrid Applications," IEEE Trans. Ind. Electron., vol. 61, no. 6, pp. 2804–2815, 2013.

[14] M. V. Gururaj and N. P. Padhy, "A Novel Decentralized Coordinated Voltage Control Scheme for Distribution System With DC Microgrid," IEEE Trans. Ind. Informatics, vol. 3203, no. c, pp. 1–1, 2017.

[15] S. Adhikari, Q. Xu, Y. Tang, and P. Wang, "Decentralized Control of DC Microgrid Clusters," pp. 567–572, 2017.

[16] P. Nuutinen, A. Lana, and T. Hakala, "Lvdc Rules – Technical Specifications for Public Lvdc Distribution Network," Cired 2017, no. June, pp. 12–15, 2017.

[17] E. Rodriguez-Diaz, F. Chen, J. C. Vasquez, J. M. Guerrero, R. Burgos, and D. Boroyevich, "Voltage-Level Selection of Future Two-Level LVdc Distribution Grids: A Compromise Between Grid Compatibiliy, Safety, and Efficiency," IEEE Electrif. Mag., vol. 4, no. 2, pp. 20–28, Jun. 2016.

[18] "ERIGrid Education-training Page." [Online]. Available: https://erigrid.eu/dissemination/.

[19] A. D. Giles, L. Reguera, and A. J. Roscoe, "Optimal Controller Gains for Inner Current Controllers in VSC Inverters," no. 4, pp. 0–5.

[20] T. Dragicevic, J. M. Guerrero, and J. C. Vasquez, "A distributed control strategy for coordination of an autonomous LVDC microgrid based on power-line signaling," IEEE Trans. Ind. Electron., vol. 61, no. 7, pp. 3313–3326, 2014.

[21] National Grid, "Testing guidance for providers of enhanced frequency response balancing service," 2017.